Can Coffee Improve Image Guidance?

Raul Wirz[*a], Ray A. Lathrop[a], Isuru S. Godage[a], Jessica Burgner-Kahrs[b], Paul T. Russell III[c], Robert J. Webster III[a,c]

[a]Department of Mechanical Engineering, Vanderbilt University, Nashville, Tennessee, USA.
[b] Center of Mechatronics (MZH), Leibniz Universität Hannover, Hannover, Germany
[c]Department of Otolaryngology, Vanderbilt University Medical Center, Nashville, Tennessee, USA.

ABSTRACT

Anecdotally, surgeons sometimes observe large errors when using image guidance in endonasal surgery. We hypothesize that one contributing factor is the possibility that operating room personnel might accidentally bump the optically tracked rigid body attached to the patient after registration has been performed. In this paper we explore the registration error at the skull base that can be induced by simulated bumping of the rigid body, and find that large errors can occur when simulated bumps are applied to the rigid body. To address this, we propose a new fixation method for the rigid body based on granular jamming (i.e. using particles like ground coffee). Our results show that our granular jamming fixation prototype reduces registration error by 28%-68% (depending on bump direction) in comparison to a standard Brainlab reference headband.

Keywords: Registration, Granular Jamming, Image-Guided Surgery, Skull Base Surgery

1. INTRODUCTION

Image guidance systems are often employed in skull base surgery. They assist the surgeon by illustrating the location of surgical tools in real time with respect to registered preoperative medical images. Accurate registration of the images to the patient is essential to enable these systems to accurately represent tool position with respect to anatomy. The accuracy of registration is measured by the Target Registration Error (TRE) at a target of interest. Yet standard TRE calculations assume a rigid connection between the bone of the patient's head and the reference rigid body tracked by the image guidance system. In practice, this connection is made using an elastic headband that is synched tight around the patient's head and to which the rigid body is attached. We illustrate using simulations in this paper that if the assumption of a rigid connection between the rigid body and the skull bone is satisfied, and errors in point measurements do not contain systematic error, clinical image guidance systems should be expected to provide very low TRE (i.e. be highly accurate)[1]. Yet anecdotally surgeons including co-author Russell report that TRE routinely reaches 5-7 mm at the skull base (this is based on visual estimates and knowledge of the dimensions of anatomical structures). Errors of this magnitude are clinically significant since the surgeon must often work closer than this to delicate and vital structures such as the optic nerves and carotid arteries. There are many possible sources of error that could explain this, including systematic errors induced by imperfect medical images and segmentation algorithms. It is also probable that the rigid body is inadvertently bumped, in some cases, after registration.

Broadly speaking, several types of registration are typically used in clinical image guidance systems[2,3,4,5]. In endonasal surgery, stereotactic frames and bone screw-based fiducial markers are typically avoided due to their invasiveness, and non-invasive surface-based registration is employed. For example, the Kolibri system of Brainlab uses points collected from the brow and areas around the eye sockets (i.e. a "browscan") to accomplish registration. After registration, the motions of the patient's head are measured by optically tracking a rigid body suspended on the patient's forehead using the elastic headband mentioned earlier. The location of the patient's head as well as the location(s) of the surgical tools are then tracked in real time by a stereo camera system that observes rigid bodies attached to each throughout the surgery. This enables the image guidance system to perform its function of showing the location of the tip of each tracked surgical tool with respect to registered preoperative images during the surgery. In endonasal sinus surgery, it is

[*] raul.wirzgo@vanderbilt.edu; phone 1 615 343-0609; http://research.vuse.vanderbilt.edu/MEDLab/

Medical Imaging 2015: Image-Guided Procedures, Robotic Interventions, and Modeling,
edited by Ziv R. Yaniv, Robert J. Webster III, Proc. of SPIE Vol. 9415, 941513
 · doi: 10.1117/12.2082965

essential to track the patient's skull, since the surgeon must be free to reposition it during surgery to achieve the best tool angles to accomplish surgery within the sinuses.

A problem arises if the rigid body attached to the patient's head moves after the registration has been accomplished, because the image guidance system assumes a rigid connection between the skull and the rigid body. However, the connection is not perfectly rigid, due to both the elasticity of the headband and the mechanical properties of the skin and other tissue surrounding the head. A previous report of 35 sinus surgery cases found movement of the headband in 14% of cases[6], indicating that better fixation methods are needed. The authors' conclusion was that registration accuracy is strongly dependent on a careful fixation of the rigid body to the patient.

To address this, in this paper we propose use of granular jamming to attach the rigid body more securely (yet still non-invasively) to the patient's skull. Granular jamming has previously been shown to be useful in the context of robot grippers for industrial applications[7], but has not previously been applied in the context of image guidance. The granular jamming concept harnesses the ability of particles to lock together when compressed and yet flow over one another when loose[8,9]. Consider vacuum packed coffee, which feels like a solid brick when sealed in its packaging. Yet as soon as the seal on the bag containing it is broken, the particles are free to flow over one another, so that the bag easily changes shape. As illustrated in Brown et al.[7] this effect can be harnessed beneficially to enable a balloon filled with coffee to conform to the shape of an object it contacts, and then solidify to pick the object up. Granular jamming has been the subject of substantial research over the past decade. It has been applied in robotic manipulation and grasping[7], haptic palpation[10,11] variable stiffness continuum robots[12], locomotion[13], and suggested for use in minimally invasive surgical devices[14]. In this paper, we use the same effect to enable a headband to conform to the patient's head and solidify to fix the rigid body used for image guidance in place with respect to the patient's anatomy.

To explore the benefits of granular jamming experimentally, in this paper we present a prototype Granular Jamming Headband (GJH), and compare its performance to standard elastic headband fixation in the presence of disturbances simulating bumping of the rigid body in the operating room. Lastly, to underscore the effect bump-based error can have in the operating room, we present the results of an experiment in which we asked the surgeon to perform drilling procedures at the skull base with the worst-case errors we observed in our disturbance experiments.

2. METHODS

2.1 Expected Accuracy of Image Guidance Systems with Random Error

To explore the effects of random error on accuracy at the skull base, we performed the following simulation. It should be noted that this simulation might not be exactly clinically accurate, due to the potential for systematic error in segmentation and imaging. However, it is informative to see whether one could potentially attribute the errors estimated by surgeons simply to random error in the registration process. To evaluate this, we segmented a computed tomography (CT) scans of a human head to develop an anatomically correct model of the geometry involved in image-guided endonasal surgery. We segmented the skull bone, skin of the patient's brow and areas around the eye sockets (i.e. the areas typically used for surface-based registration in clinical image guidance systems), as well as the sphenoid sinus and pituitary gland. The sphenoid and pituitary represent anatomical locations at the skull base where drilling and other surgical procedures are often performed, and we will use them as targets to evaluate TRE.

To explore in simulation whether accurate registrations at the skull base can be accomplished with varying levels of error in the collection of skin surface points for registration, we sampled points from the segmented facial surfaces and the sphenoid sinus. We first obtained large set of just over fifteen thousand points on the segmented facial surfaces typically used for registration, namely the surfaces along the cheek bones and brow ridge (see Figure 1 for a visual depiction of this "registration point set"), and we similarly obtained a set of just under three thousand surface points from the face of the sphenoid sinus nearest the nose, constituting the "target point set". Both point sets are generated from the vertices of the triangulated surface obtained from segmentation.

To explore the accuracy in surface-based registration, we sampled 200 random points from the registration point set and simulated the intraoperative measurement by perturbing each point with the varying levels of fiducial localization error (FLE) which we assumed here to be random, normally distributed, and zero-mean. Thus, we perturbed the points by using the sum of two 3x3 covariance matrices, where the diagonal components are the variances of the independent components of the FLE along each principal axis:

$$p_{perturb} = \left(\begin{bmatrix} 0.01 & 0 & 0 \\ 0 & 0.01 & 0 \\ 0 & 0 & 0.09 \end{bmatrix} + \begin{bmatrix} (3+\sigma)^2 & 0 & 0 \\ 0 & (3+\sigma)^2 & 0 \\ 0 & 0 & (3+\sigma)^2 \end{bmatrix} \right) p_i ,$$

where the first covariance matrix accounts for anisotropic FLE of the tracker with RMS 0.33 mm and the second covariance matrix accounts for other error which is assumed isotropic with σ in a range of [0, 5] mm plus a maximum of 3 mm of error due to the air-skin surface segmentation[2], and p is a point drawn from the registration point set. This FLE is a Gaussian model that is intended to include the error associated with the optical tracker, as well as the error associated with skin deformation, and the imaging/segmentation process. We then performed Iterative Closest Point[15] (ICP) registration to compute the transformation matrix T_{reg} between the perturbed registration points and the CT scan surface model. We performed this procedure 100 times, each with an initial random initial transformation between the segmented CT scan surface and the randomly sampled registration point sets (200) for increments of RMS_{FLE}. The random transformation is determined by 3 randomly generated Euler angles in the range of [0, 2Π] rad for the rotation and by a randomly generated 3x1 translation vector with components in the range of [0, 1000] mm. The FLE introduced was selected at various levels in a range of [0.33, (0.33+3+5)] mm, with 0.33 mm as the minimum expected FLE from the optical tracker in presence of no further errors. TRE was calculated according to:

$$\text{TRE} = \sqrt{\frac{1}{n}\sum_{i=1}^{n} \left\| T_{\Delta} p_i - p_i \right\|^2} ,$$

with $T_{\Delta}=T_{GT}^{-1}T_{reg}$ describing the difference between the ground truth registration and the computed registration and p out of the target point set.

The results of this simulation study are presented in Section 3.1. They illustrate that the fiducial localization error must be high before TRE suffers substantially, if it contains only random error. Thus, this simulation supports the idea that random error alone cannot describe the errors surgeons see in the operating room. Based on this, we believe that the culprit is likely either (1) systematic (i.e. non-random) error, (2) registration being performed incorrectly by clinical personnel, or (3) unmodeled motion between the rigid body and the skull. In the remainder of this paper we focus on solutions to mitigate (3).

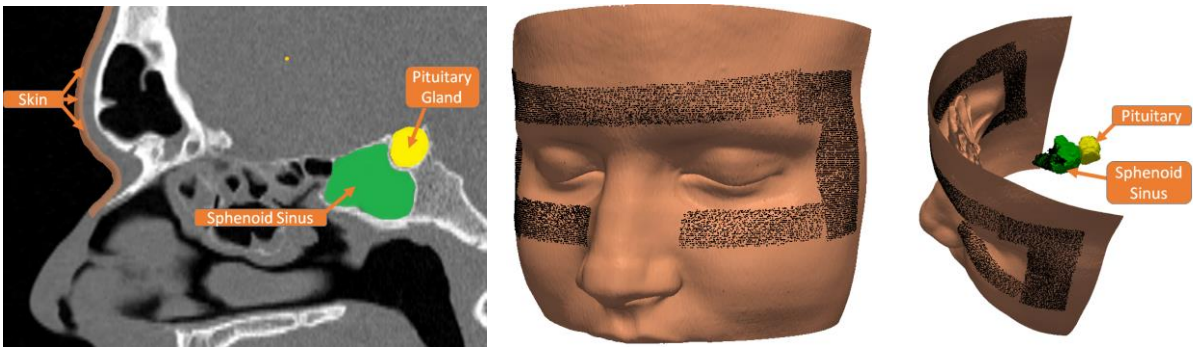

Figure 1. (Left) A sagittal view of the patient with the skin area used for registration indicated, and the example skull base target zones illustrated. (Center) Black dots on the facial surface illustrating the registration point set. (Right) A 3D model of the segmented objects of interest.

2.2 Potential Error Due to Skin Mobility

Since many clinical personnel (including our collaborators) are careful with image guidance system setup, and collect points according to the manufacturer's specifications, we believe that a likely culprit in cases of large registration error is unmodeled motion between the rigid body and the skull. This is a reasonable hypothesis, since it has previously been experimentally shown that skin mobility with respect to the skull bone can range from 1.3–13.1 mm, with a mean of 5.34 ± 2.65 mm under load[16]. Figure 2 illustrates two ways loads can be applied to the skin that would cause relative motion between the optical tracking rigid body and the patient's skull. We use as an example the optical tracking fixation system

of the Brainlab Kolibri system, which uses a stiff elastic headband secured with Velcro to affix the rigid body around the patient's head. We have observed two ways in which the rigid body can shift after attachment to the patient. One is that clinical personnel or equipment can inadvertently bump the optical tracking rigid body. Another is that the process of repositioning the patient's head can apply loads to the back of the elastic headband where the patient's head is supported by a pillow on the operating table causing the entire band to apply rotational forces to the skin around the patient's head. We have not observed noticeable relative motion between the band and the skin, but we do believe that skin mobility relative to the skull can move both skin and band together relative to the skull.

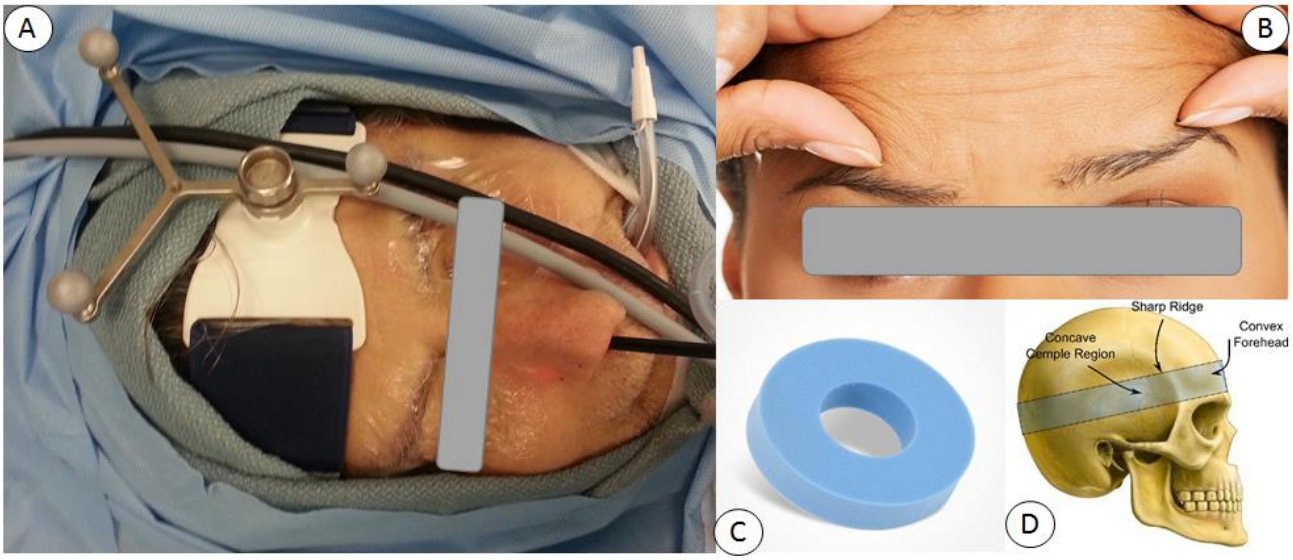

Figure 2. Possible causes of error due to skin mobility. (A) Operating room personnel can accidentally bump the rigid body after registration with their hands or with other pieces of equipment like the cords illustrated. (B) An illustration of skin mobility relative to the skull, (C) A foam pillow used to support the patient's head. (D) An illustration of the way the band wraps around the patient's head – as the head is repositioned during surgery, the pillow and surgical table can apply lateral loads to the back of the band, which can transmit loads around the head and ultimately move the optically tracked rigid body relative to the skull.

2.3 A Better Fixation System: Granular Jamming

We propose granular jamming as a way to create a fixation system that is less susceptible to skin mobility. We designed a prototype Granular Jamming Headband (GJH) to test this hypothesis (Figure 3). We designed it to be compatible with current clinical image guidance systems, meaning that it should hold the rigid body at roughly the same location as the current headband, and leave the brow area free for brow scan registration. These choices were made with the goal of facilitating both regulatory approval and adoption by clinical personnel.

The GJH prototype (Figure3-Left) consists of four major parts: a c-shaped plastic forehead shield (Figure3-Left-A), an elastic strap to secure it to the patient's forehead (Figure3-Left-C), two granular jamming pads positioned under the shield at the patient's temples (Figure3-Left-B), and a vacuum apparatus consisting of tubes and a vacuum pump (Figure3-Left-D). The plastic forehead shield is made from high-density polyethylene and is 6 mm thick and 80 mm tall. It is semi-flexible such that it applies light pressure to the granular jamming pads when placed on the forehead, yet has the elasticity to adjust to various sized heads. The elastic strap is attached to the ends of the shield just behind the patient's temples. The strap wraps around the back of the head to prevent the band from pulling forward and away from the patient's forehead. Two granular jamming pads are attached to the inside of the shield and conform to the patient's temples when the shield is put in place. When a vacuum is applied to the pads they solidify, molding themselves to the patient's skull contours and holding the shield firmly in place.

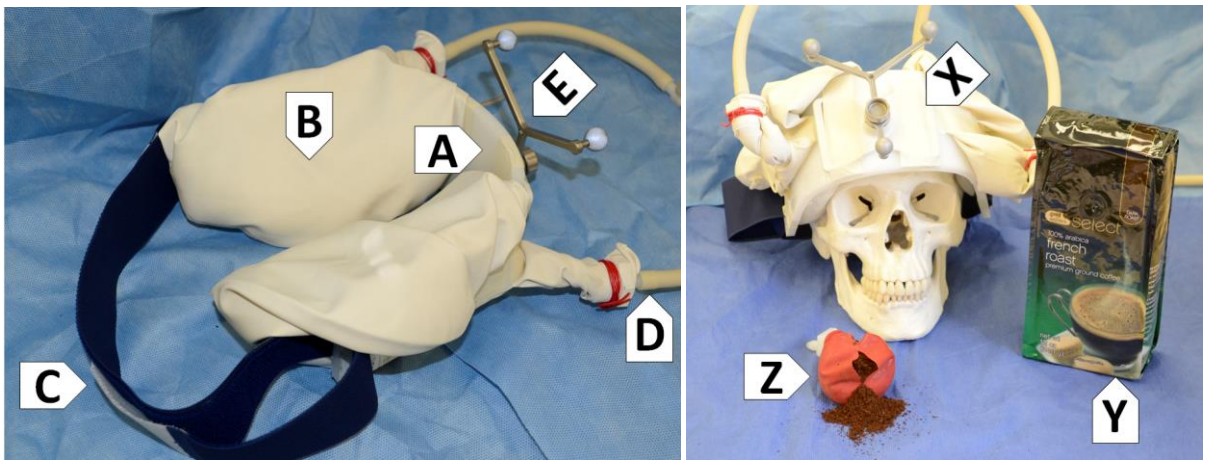

Figure 3. Our new Granular Jamming Headband (GJH) uses ground coffee (Z) within a balloon (B) to conform to the patient's head. The GJH then provides rigid, yet non-invasive fixation to the patient's skull when a vacuum is drawn on the balloon, causing the coffee to jam and solidify within the balloon. (A) A plastic forehead shield lightly presses the granular jamming pads (i.e. coffee-filled balloons) against the patient's temples, (B) a granular jamming pad (C) the elastic band that pulls the forehead shield snugly against the patient's forehead before the vacuum is activated, (D) a vacuum tube leading to the vacuum pump (not shown), (E) the rigid body tracked by the image guidance system, (X) front view of the GJH mounted on a skull, (Y) a bag of vacuum packed coffee from the supermarket illustrating how solid coffee can be solid when vacuum packed.

To analyze the performance of the GJH in comparison to a standard Brainlab headband we conducted an experiment in which force perturbations simulating bumps are applied and released to the rigid body. To carry out the experiment, we used an NDI Polaris Spectra optical tracker to track (1) the rigid body attached to the patient's forehead by either the Brainlab headband or the new GJH, and (2) a rigid body attached to the patient's teeth using a bite-block (this serves as ground truth, since the teeth will not move with respect to the skull, and the bite block can be secured well to the teeth). A tracked point probe was also used to take three reference points in the skull (the right tragus, the left tragus and the glabella) in order to estimate the location of the skull base with respect to the ground truth bite block. Note that errors in estimating the location of the skull base with respect to the ground truth bite block frame are not particularly important here – there is no need to be exact. All we need is to establish a target point in the bite block frame for TRE calculation. What we are really measuring is the difference in position and orientation between the two tracked rigid bodies. But it is useful to have some estimate of the location of the skull base in the bite block frame to use for TRE calculation, so that our results can be intuitively understood in terms of clinically representative error at the skull base.

To test each fixation system, we will apply external forces to simulate bumping to the rigid body in various directions. This will be accomplished using 9.81 N applied in four directions with respect the patient's face: up, down, left and right. The results of this experiment are reported in Section 3.2.

2.4 The Consequences of Bump-Induced Registration Error

To underscore the potential consequences of bump-induced registration error, we performed a drilling experiment with the average registration error identified in our simulated bumping experiment. In this experiment, an experienced skull base surgeon (co-author Russell) was asked to drill out a simulated hard tumor inside the sphenoid sinus. He performed this procedure twice, using two identical plastic phantom models. To generate models, we segmented the relevant portions of the skull from a CT scan as described in Section 2.1. We then 3D printed the resulting shapes to obtain the model shown in Figure 4, which was made in Acrylonitrile butadiene styrene (ABS) on Stratasys Dimension SST 768. The sphenoid sinus in this phantom was filled in with solid plastic to simulate a hard tumor. The total tumor volume was 7895 mm^3.

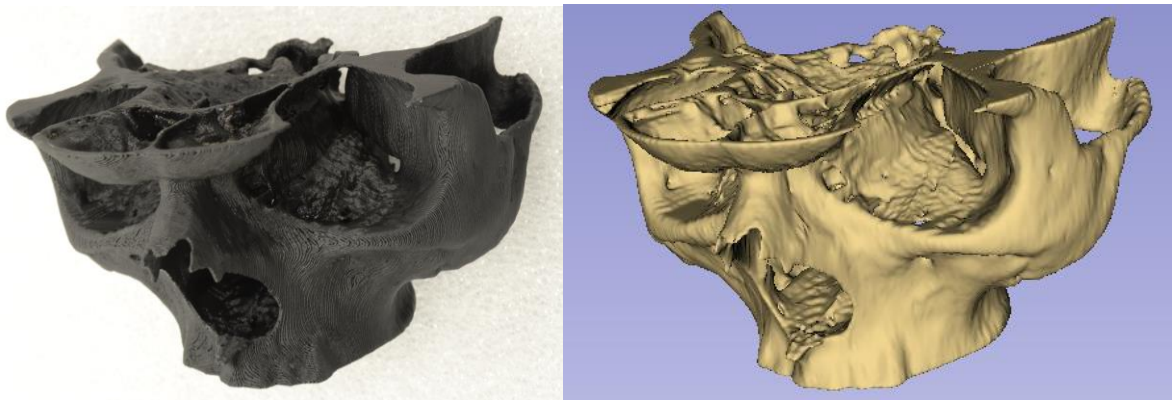

Figure 4. A photograph of the phantom used (Left) in our drilling experiments, which was created via 3D printing from a segmented CT scan (Right). The phantom was registered using point based registration with identifiable landmarks, and held rigidly in place during drilling, so no optically tracked rigid body was required.

Two identical copies of the phantom shown in Figure 4 were 3D printed. One was used in an experiment simulating the elastic headband, and the other in an experiment simulating the GJH. In both experiments, the surgeon was equipped with a surgical drill, an endoscope, a suction tube, a tracked probe and an image guidance system (IGS). The IGS was created using 3D Slicer with SlicerIGT, using a Polaris Spectra optical tracker (Northern Digital, Inc.).

The experiment was designed to explore the effects on drilling by the surgeon of errors in registration induced by the bumping of the optically tracked rigid body. To simulate bumping, the image guidance system was initialized with no errors at the beginning of the drilling procedure. Then, part way through the procedure (approximately 5 minutes after drilling began), without the surgeon's knowledge the optical tracking rigid body was perturbed (in software) by the amount of the maximum perturbation found in our simulated bumping study. We performed this experiment twice, once on each phantom, one using the average Brainlab headband perturbation, and again using the average GJH perturbation, from Table 1. In both experiments, the surgeon had to rely to a large degree on the IGS system, since the tumor and surrounding bone were printed using the same material, meaning that there were no visual cues for the surgeon indicating where the tumor ended and bone began. The surgeon's task was to drill out the entire tumor and none of the bone. The sphenoid sinus was selected because it is in close proximity to structures to which damage induces serious complications (or even death), including the internal carotid artery, the brain, and the optic nerve.

To evaluate the results of the drilling experiment, a tracked conoscopic holography distance measurement device (ConoProbe Mark 3.0, Optimet Metrology Inc.)[17,18,19] was used to scan the inside of the cavity after the surgeon had completed the drilling. Since the calibrated ConoProbe was optically tracked using the same tracking system used by the surgeon for IGS, it is registered to anatomy in exactly the same way the surgeon's tools, enabling us to obtain high quality measurements of the drilled cavity. To assess fidelity of the drilled cavity compared to the planned cavity, we will compare their volumes. The results of this experiment are discussed in Section 3.3.

3. RESULTS

3.1 Expected Accuracy of Clinical IGS Systems: Simulation Results

In this experiment we conducted simulations with various levels of fiducial localization error in the registration point set, to see how much error was necessary before the TRE at the skull base reached 1 mm, assuming only random, normally distributed errors with zero-mean components are present in the system. This study is not intended to be a perfect representation of the clinical environment, where systematic errors in registration points may occur. But it does answer the question of whether errors surgeons estimate that they see can be explained solely by random error. Figure 5-Right illustrates an example sampled set of points from the registration point set, with the maximum error σ of 5 mm introduced. This example had the highest level of error in the cases we investigated in our simulation.

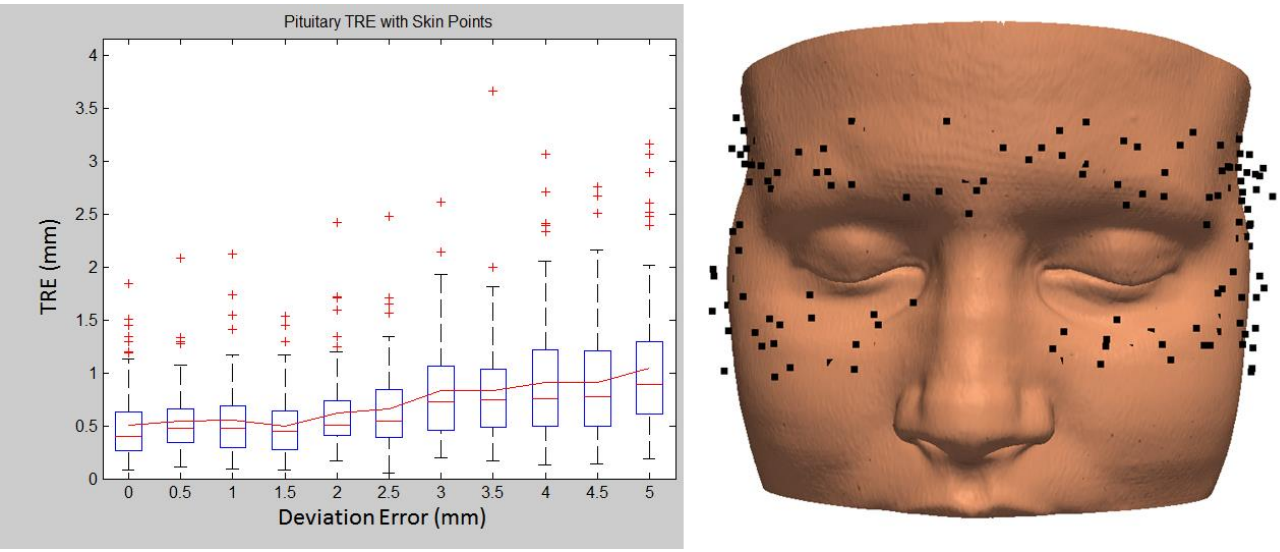

Figure 5. (Left) Results for the pituitary gland TRE, where the edges of the box are the 25th and the 75th percentiles, the central red line in the box is the median, the red crosses are points outside the 75th percentile, and the red line connecting the boxes is a plot of the mean. (Right) Frontal view of the face and the 200 random points chosen from the surface with the worst-case error of 5 mm introduced (recall that an additional 3.33 mm random error is also included to model tracker error as well as skin deformation error, as discussed in Section 2.1, making the total random error shown in the points in the figure 8.33 mm).

The results of each different FLE value can be observed in Figure 5, which show that the mean TRE is about 0.5 mm when the surface points are only perturbed by the minimum FLE. This simulation illustrates that unmodeled effects are responsible for instances of large TRE at the skull base. It seems reasonable that one of these is potential motion of the rigid body relative to the skull, in some cases. Thus, we will next compare the standard Brainlab headband with our new GJH in the presence of simulated bumping that takes place after registration to determine (1) the magnitude of errors that can be induced by bumping with standard fixation, and (2) whether the GJH can reduce them.

3.2 Simulated Bumping Experiment

In this experiment we attached the fixation device to a person's head and applied loads in various directions. The loads were applied by pulling on a string attached to the center of the rigid body with a spring scale with a force of 9.18 N. We applied the force and then released it, after which we measured the positions of the rigid bodies. We conducted this experiment (see Figure 6) twice, once with the Brainlab headband and once with the GJH. In both cases, the locations of the bite block frame and forehead-mounted frame were recorded using the optical tracker, after each simulated bump, and compared to the frame's location before the bump. The target of interest at the skull base was selected as described in Section 2.3.

Figure 6. Illustration of the bite block and GJH attached to the subject's head before the simulated bumps were applied. The Brainlab headband is shown in Figure 2.

Table 1 lists the TRE results obtained for the Brainlab commercial elastic headband and the new granular jamming headband. These results illustrate that the GJH is more robust to force perturbations than the Brainlab headband.

Table 1. TRE determined in simulated bumping experiments.

Force Direction	*Headband*	*Granular Jamming Headband (GJH)*
Right	4.69 mm	2.75 mm
Left	5.19 mm	3.52 mm
Up	4.14 mm	1.26 mm
Down	5.70 mm	1.61 mm

3.3 Experimental Results on Drilling With Bump-Induced Registration Error

We performed the experiment described in Section 2.4. The experimental setup was as shown in Figure 7.

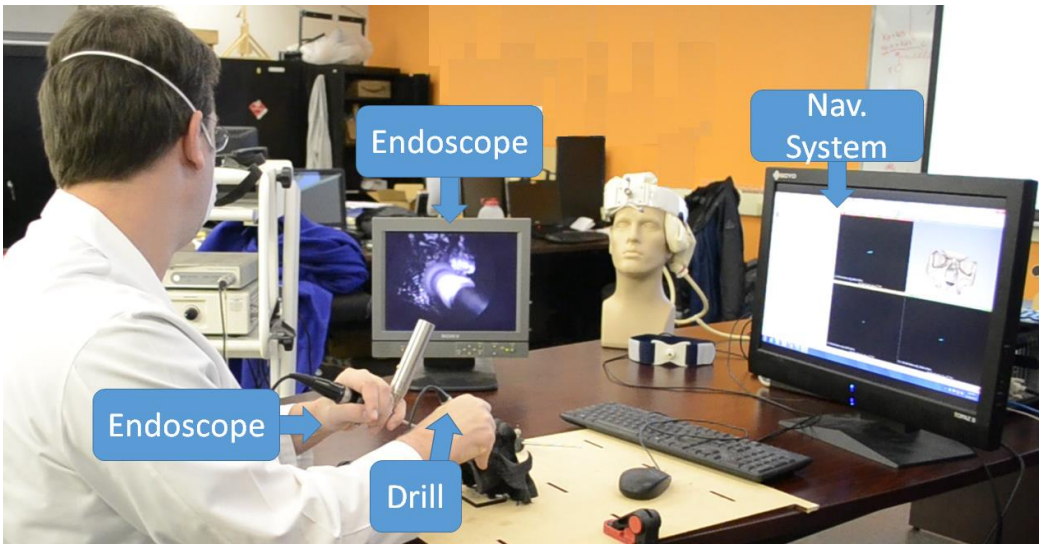

Figure 7. Experimental setup for the drilling experiment evaluating the effects of registration error on the surgeon.

In normal clinical drilling, the surgeon begins with a rough check of guidance system accuracy using a tracked probe to touch known landmark locations on the skull. In a clinical case, if the accuracy is not satisfactory for the surgeon, he will obtain a new registration. In both experiments, the initial TRE was less than 1 mm and was deemed satisfactory by the surgeon (it was 0.58 mm for the headband case, and 0.79 for the GJH case). After this verification, the surgeon drilled as he typically does in clinical cases. He first used the tracked probe to localize the target area to be drilled, then mentally estimated the direction and depth to drill, and finally drilled out the target area. Lastly, the surgeon verified that the drilled area was as intended using the tracked probe to touch points on the drilled surface, and then drilled again (if needed) to reshape the surface until the drilled volume matched the surgeon's initial plan to the surgeon's satisfaction. In doing this drilling, since the sphenoid sinus was filled with simulated bone, the surgeon was forced to rely on image guidance rather than bone features to ensure that he was drilling in the correct location, as intended.

The surgeon repeated the same procedure twice, once using the average TRE from the headband and again using the average TRE from the GJH. In both cases, the drilling began with a TRE below one millimeter but after 5 minutes of drilling, without the surgeon's knowledge, the TRE of the image guidance system was increased to 5.47 mm for the headband (determined by adding the initial 0.58 mm plus 4.89 mm simulating an average bump) for the elastic headband. In the GJH experiment 3.53 mm TRE was introduced into the IGS display (determined by adding the initial 0.79 mm plus 2.74 mm simulating an average bump) for the GJH device. The TRE was changed to these levels by moving (in software) the locations of landmarks 1 and 2 (the two leftmost in Figure 8-Right) in a direction perpendicular to the coronal plane, and into the head. These landmarks were moved far enough that the TRE at the skull base changed in the amount indicated previously. These changes were noticeable to the surgeon and he began to take a more conservative approach to the drilling. This included looking for anatomical landmarks outside the sphenoid sinus to help him orient himself. In Figure 8-Left, the deterioration of the TRE can be observed in that the IGS system shows that the probe was inside the pituitary gland, even though the real probe was touching the bone.

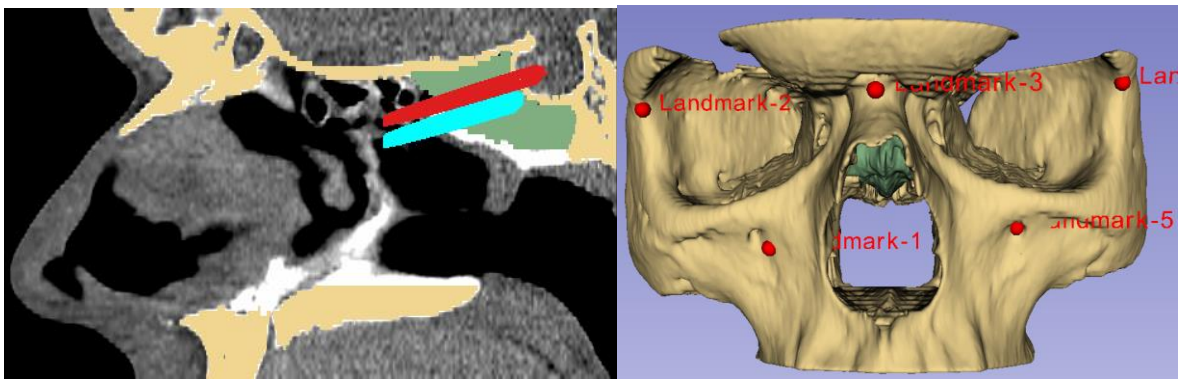

Figure 8. (Left) An example of what happens when a TRE of 5.47 mm is present in the system. The blue figure shows the true probe location, touching the bone. The red figure shows the location of the probe with a TRE of 5.47 mm, in the pituitary gland area. (Right) An illustration of the five landmark positions used (red spheres) to register the phantom to the image guidance system.

Once the surgeon finished drilling, we compared the drilled volume to the planned drill volume (namely the entire interior of the sphenoid sinus). To do this, as described in Section 2.4, we used a calibrated, tracked ConoProbe to obtain a laser scan of the interior of the resection volume. Figure 9 illustrates our measurement technique. First the calibrated ConoProbe was used to capture surface points from the facial bones (for registration – see Figure 9-A) and from the drilled area in the sphenoid sinus. A total of 2500 points were captured with the ConoProbe (Figure 9-B). Using the facial points, we performed a surface registration using the Iterative Closest Point (ICP) algorithm[15] enabling us to register the locations of the sphenoid points to the segmented CT scan model used to print the phantoms (Figure 9-C). We then used the Poisson Surface Reconstruction[20] algorithm to generate a mesh from the sphenoid point cloud (Figure 9-D). This mesh defines the boundary where the drilling by the surgeon ended. Using this mesh, we compute the percentage of the target area that was left behind by the surgeon, which consists of all the material above the mesh.

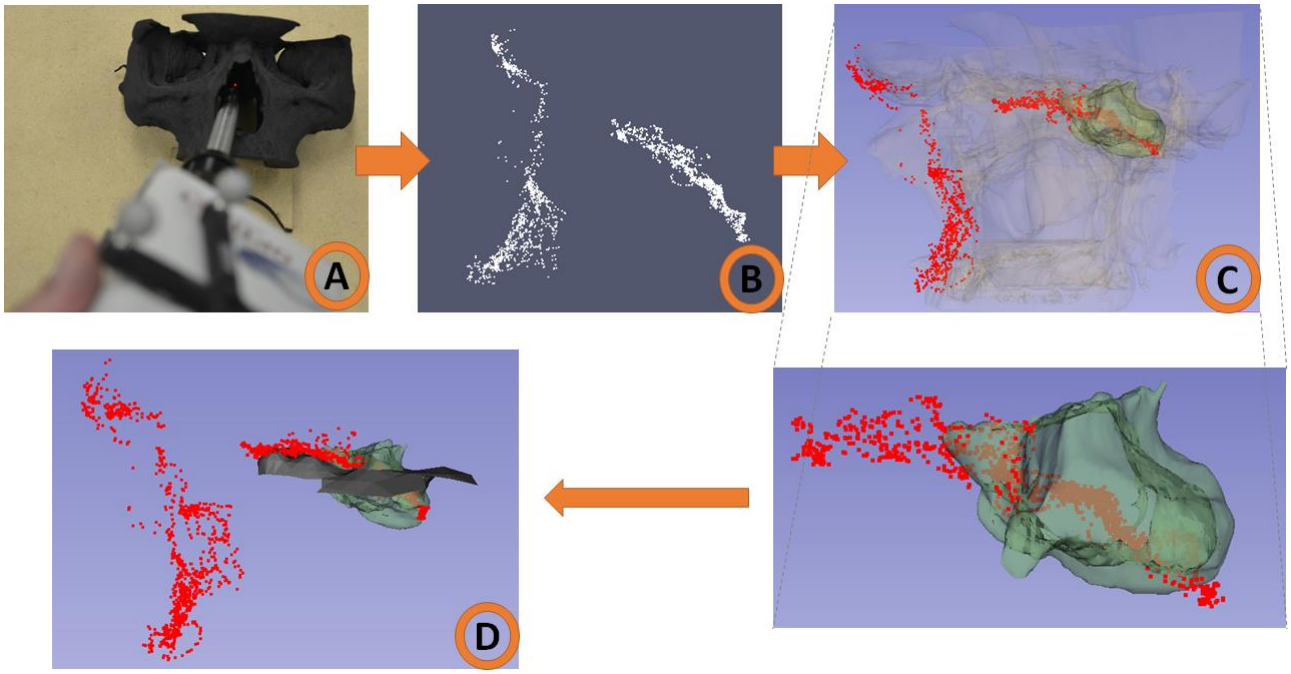

Figure 9. The volume drilled was calculated by: (A) Capturing the drilled tumor surface points with the ConoProbe (which are illustrated in (B)), (C) using the Iterative Closest Point algorithm to register the physical model to the virtual model, and (D) generating the mesh with the Poisson Surface Reconstruction algorithm.

The results are shown in Table 2, which illustrates that the lower errors provided by the GJH when bumped enabled the surgeon to drill out more of the target region. In both cases, the surgeon's conservative approach can be observed, in that he did not attempt to drill the entire region once he realized that he could not trust the image guidance display. The surgeon drilled less total volume in the case of the headband, stopping when he perceived he was close to violating a critical structure such as the brain or carotid artery. The original tumor volume was 7895 mm^3 and the drilled volume of tumor was 5770 mm^3 for the GJH and 2604 mm^3 for the headband. This conservative behavior can be also observed in the time needed to complete the drilling, where the surgeon was slower and more careful when more error was introduced.

Table 2. Comparison results between the two drills

Case	*Surgery Time*	*Initial TRE*	*Final TRE*	*Volume resected*	*Total*
Headband	20 min	0.58 mm	5.47 mm	2604 mm^3	32.98%
GJH	15 min	0.79 mm	3.53 mm	5770 mm^3	73.07%

4. CONCLUSIONS

In this paper, we have shown that commercial elastic headbands can yield large errors when subjected to unplanned perturbations or "bumps" by operating room staff after registration has been established via brow scan. We have also proposed a novel solution to the non-invasive fixation problem, borrowing the idea of granular jamming from the field of robotics and applying it to create a new Granular Jamming Headband (GJH), which we showed can reduce errors by 28%-68% in the presence of perturbations representing bumping of the rigid body by operating room staff. The GJH uses coffee grounds that conform to the patient's skull and solidify when a vacuum is drawn on the elastic bag containing them. We also proposed in this paper that skin mobility is a reasonable explanation for large errors noted by surgeons in some clinical cases, since it can potentially cause the optically tracked rigid body to shift relative to the skull.

This is the first use of granular jamming in an image guidance system of which we are aware. This approach has the potential to make image guidance systems more robust to the perturbations they may experience in real-world operating rooms, and thus make them safer for patients and more reliable for surgeons. In future work, we intend to construct additional prototypes optimizing the parameters of the granular jamming pads, as well as the frame that holds them. We believe that a device of this type has the potential to make image guidance systems more robust, and thereby enable doctors to trust them more than they are able to today. This may ultimately result in safer, more accurate, and more efficient surgeries for patients undergoing endonasal surgery.

5. ACKNOWLEDGEMENTS

This research was supported by the National Institutes of Health under grant number R01 EB017467. The content is solely the responsibility of the authors and does not necessarily represent the official views of the National Institutes of Health.

REFERENCES

[1] Labadie, R. F., Davis, B. M.., Fitzpatrick, J. M., "Image-guided surgery: what is the accuracy?," Current opinion in otolaryngology & head and neck surgery **13**(1), 27–31 (2005).

[2] Fitzpatrick, J. M., "The role of registration in accurate surgical guidance.," Proceedings of the Institution of Mechanical Engineers. Part H, Journal of engineering in medicine **224**(5), 607–622 (2010).

[3] Widmann, G., "Image-guided surgery and medical robotics in the cranial area.," Biomedical imaging and intervention journal **3**(1), e11 (2007).

[4] Mascott, C. R., Sol, J.-C., Bousquet, P., Lagarrigue, J., Lazorthes, Y.., Lauwers-Cances, V., "Quantification of true in vivo (application) accuracy in cranial image-guided surgery: influence of mode of patient registration.," Neurosurgery **59**(1 Suppl 1), ONS146–ONS156; discussion ONS146–ONS156 (2006).

[5] Metzger, M. C., Rafii, A., Holhweg-Majert, B., Pham, A. M.., Strong, B., "Comparison of 4 registration strategies for computer-aided maxillofacial surgery.," Otolaryngology--head and neck surgery : official journal of American Academy of Otolaryngology-Head and Neck Surgery **137**(1), 93–99 (2007).

[6] Lorenz, K. J., Frühwald, S.., Maier, H., "[The use of the BrainLAB Kolibri navigation system in endoscopic paranasal sinus surgery under local anaesthesia. An analysis of 35 cases].," HNO **54**(11), 851–860 (2006).

[7] Brown, E., Rodenberg, N., Amend, J., Mozeika, A., Steltz, E., Zakin, M. R., Lipson, H.., Jaeger, H. M., "Universal robotic gripper based on the jamming of granular material," Proceedings of the National Academy of Sciences (2010).

[8] Liu, A. J.., Nagel, S. R., "Nonlinear dynamics: Jamming is not just cool any more," Nature **396**(6706), 21–22 (1998).

[9] Jaeger, H. M., "Celebrating Soft Matter{'}s 10th Anniversary: Toward jamming by design," Soft Matter, -, The Royal Society of Chemistry (2015).

[10] Li, M., Ranzani, T., Sareh, S., Seneviratne, L. D., Dasgupta, P., Wurdemann, H. A.., Althoefer, K., "Multi-fingered haptic palpation utilizing granular jamming stiffness feedback actuators," Smart Materials and Structures **23**(9), 95007, IOP Publishing (2014).

[11] Stanley, A. A., Gwilliam, J. C.., Okamura, A. M., "Haptic jamming: A deformable geometry, variable stiffness tactile display using pneumatics and particle jamming," 2013 World Haptics Conference (WHC), 25–30, IEEE (2013).

[12] Cheng, N. G., Lobovsky, M. B., Keating, S. J., Setapen, A. M., Gero, K. I., Hosoi, A. E.., Iagnemma, K. D., "Design and Analysis of a Robust, Low-cost, Highly Articulated manipulator enabled by jamming of granular media," 2012 IEEE International Conference on Robotics and Automation, 4328–4333, IEEE (2012).

[13] Steltz, E., Mozeika, A., Rodenberg, N., Brown, E.., Jaeger, H. M., "Jsel: Jamming skin enabled locomotion," Intelligent Robots and Systems, 2009. IROS 2009. IEEE/RSJ International Conference on, 5672–5677 (2009).

[14] Jiang, A., Xynogalas, G., Dasgupta, P., Althoefer, K.., Nanayakkara, T., "Design of a variable stiffness flexible manipulator with composite granular jamming and membrane coupling," Intelligent Robots and Systems (IROS), 2012 IEEE/RSJ International Conference on, 2922–2927 (2012).

[15] Besl, P. J.., McKay, H. D., "A method for registration of 3-D shapes," IEEE Transactions on Pattern Analysis and Machine Intelligence **14**(2), 239–256, IEEE Computer Society (1992).

[16] Mitsui, T., Fujii, M., Tsuzaka, M., Hayashi, Y., Asahina, Y.., Wakabayashi, T., "Skin shift and its effect on navigation accuracy in image-guided neurosurgery.," Radiological physics and technology **4**(1), 37–42 (2011).

[17] Burgner, J., Simpson, A. L., Fitzpatrick, J. M., Lathrop, R. A., Herrell, S. D., Miga, M. I.., Webster, R. J., "A study on the theoretical and practical accuracy of conoscopic holography-based surface measurements: toward image registration in minimally invasive surgery.," The international journal of medical robotics + computer assisted surgery : MRCAS **9**(2), 190–203 (2013).

[18] Simpson, A. L., Burgner, J., Glisson, C. L., Herrell, S. D., Ma, B., Pheiffer, T. S., Webster, R. J.., Miga, M. I., "Comparison study of intraoperative surface acquisition methods for surgical navigation.," IEEE transactions on bio-medical engineering **60**(4), 1090–1099 (2013).

[19] Lathrop, R. A., Hackworth, D. M.., Webster, R. J., "Minimally invasive holographic surface scanning for soft-tissue image registration.," IEEE transactions on bio-medical engineering **57**(6), 1497–1506 (2010).

[20] Kazhdan, M., Bolitho, M.., Hoppe, H., "Poisson surface reconstruction," Proceedings of the fourth Eurographics symposium on Geometry processing (2006).